PHYSICAL REVIEW A **72**, 050701(R) (2005)

High-charge-state formation following inner-shell photodetachment from S^-

R. C. Bilodeau,[1,2] N. D. Gibson,[3] J. D. Bozek,[2] C. W. Walter,[3] G. D. Ackerman,[2] P. Andersson,[4] J. G. Heredia,[1,2] M. Perri,[1,2] and N. Berrah[1]

[1]*Physics Department, Western Michigan University, Kalamazoo, Michigan 49008-5151, USA*

[2]*Advanced Light Source, Lawrence Berkeley National Laboratory, Berkeley, California 94720, USA*

[3]*Department of Physics and Astronomy, Denison University, Granville, Ohio 43023, USA*

[4]*Department of Physics, Göteborg University, SE-412 96 Göteborg, Sweden*

(Received 12 August 2005; published 2 November 2005)

The formation of S^+, S^{2+}, S^{3+}, and S^{4+} is observed following inner-shell photodetachment of S^-. The photodetachment spectra for all possible ionic products are obtained over a large region of photon energies covering both the $2p$ and $2s$ thresholds (S^{5+}, is energetically allowed at the higher photon energies, but not observed), and are placed on an absolute scale. The $2s$ threshold energy is measured to be 224.6(5) eV, allowing the determination of the neutral atomic S $2s^{-1}3s^23p^5$ inner-shell excited state energy for the first time. The S^- $2s^{-1}3s^23p^6$ $^2S_{1/2}$ state is observed as a Feshbach resonance 2.3(5) eV below the $2s$ threshold in the S^+, S^{2+}, and S^{3+} product channels.

DOI: 10.1103/PhysRevA.72.050701 PACS number(s): 32.80.Gc, 32.80.Hd

Negative ions are of fundamental interest, in addition to being important in a number of physical processes (e.g., stellar atmospheres, molecular clouds, atomic mass spectrometry, and plasma physics [1]). The interest stems in part from the qualitatively different features of the short-ranged potential that binds atomic negative ions, and from the theoretical challenges posed by the strong electron correlation effects present in these systems. Prior to 2001, experimental investigations of negative ions were limited to the valence electrons, mainly employing laser-based photodetachment techniques (for recent reviews see Ref. [2]). Recently, however, inner-shell photodetachment of negative ions utilizing intense vacuum ultraviolet (VUV) sources has become accessible, and has attracted considerable theoretical [3] and experimental interest ([2,4–8], and references therein).

In a very recent publication [6] we studied inner-shell photodetachment threshold laws in He^- $1s$ and S^- $2p$ photodetachment, and observed good agreement with the Wigner threshold law [9]. In that study, we obtained an apparent $2p$ threshold energy for S^- of 161.04(6) eV [errors are 1 standard deviation (SD) throughout]. We investigate here inner-shell photodetachment of S^- over a much larger range of photon energies, from below the $2p$ threshold to well above the $2s$ threshold. All ionic products energetically allowed over this range are detected, i.e., a total of up to five electrons removed (S^{5+}, possibly produced at the higher photon energies, is not observed). Charge states higher than +1 have only previously been observed in inner-shell photodetachment of much heavier negative ions; up to 3 and 4 total electron emission was detected in $4d$ photodetachment of Te^- [7] and I^- [8], respectively. In those cases, higher charge state production was attributed mainly to sequential (cascade) Auger decay processes, while in the present case we argue that higher order processes such as simultaneous multi-Auger decay must dominate. Finally, we measure the $2s$ near-threshold region to high detail, and observe for the first time the $2s \rightarrow 3p$ Feshbach resonance resulting from the S^- $2s^{-1}3s^23p^6$ $^2S_{1/2}$ state, found to be bound by 2.3(5) eV below the $2s$ threshold. In striking contrast to Te^-, where a similar filling of the $2p$ shell resulted in a Feshbach resonance observed only in the Te^+ channel [7], the resonance in S^- is clearly seen to couple strongly into the S^+, S^{2+}, and S^{3+} product channels.

The experiments were performed using the ion-photon beamline [10] at the Advanced Light Source (ALS). A 9.96 keV, ≈350 nA beam of S^- $3s^23p^5$ ^2P was extracted from a cesium sputter source and merged with a counter-propagating photon beam from ALS beamline 10.0.1. The photon-ion interaction in the merged region lead to a net loss of 2 or more electrons. The resulting S^{n+} ions (the signal) were deflected by a demerging magnetic field and counted using an multichannel plate based detector.

Different final product charge states are easily identified and separated with the magnetic and electric fields in the detection stage of the apparatus. For photon energies higher than 117.79 eV it is energetically possible to remove up to five valence electrons from S^-, to form charge states up to S^{4+} [11,12]. All of these charge states were observed in the experiment. Although it is energetically possible to remove a sixth electron beyond 190.38 eV, S^{5+} was not observed. Since detection of neutral products is not possible with the current apparatus, neutral S atoms could not be monitored.

Figure 1 shows the signal observed in the S^+, S^{2+}, S^{3+}, and S^{4+} product channels following $2p$ and $2s$ photodetachment or excitation of S^-. The signal has been scaled to the measured absolute cross sections using a method similar to previous experiments with this apparatus [4,10]. Given the target-ion current, velocity, and charge, I, v, and q, respectively, the cross section σ is obtained from the signal rate R and photon flux Φ through $\sigma = qvR/I\Phi F$, where the form factor F is a measure of the quality of the overlap between the ion and photon beams. The signal rate is $R = R_0/\Omega_{det}\Omega_{elect}$, given the observed count rate R_0, the detector efficiency Ω_{det}, and the electronics pulse efficiency Ω_{elect}. In the present experiment Ω_{det} was measured to be 0.654(23) for S^+ and assumed to be 0.95(5) and 0.98(2) for S^{2+} and S^{3+}, respectively [13]. Ω_{elect} was measured to be

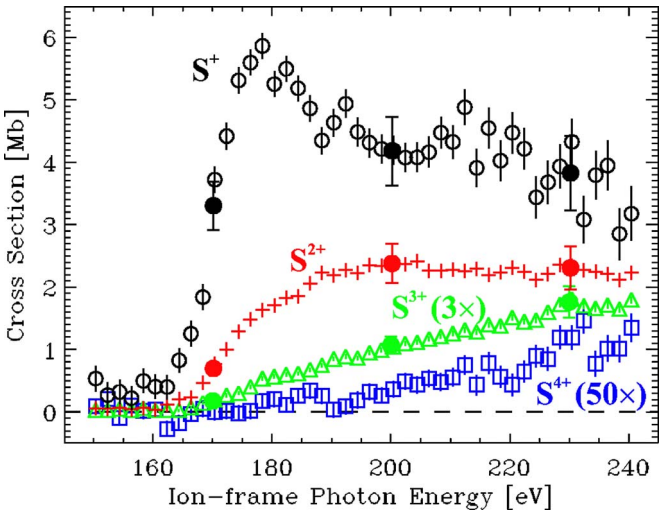

FIG. 1. (Color online) Observed S^+ (◯), S^{2+} (+), S^{3+} (△), and S^{4+} (□) production following photoabsorption in S^-, scaled to measured absolute cross sections (filled circles, see Table II). For presentation purposes, S^{3+} and S^{4+} signals have been magnified by a factor of 3 and 50, respectively.

0.75 to 0.91, depending on the detected charge state and the electronics settings.

The main instrumental uncertainties in the cross section measurements arise from the photon flux determination (±7.1% to 11.5%), the signal (S^{n+}) collection and detection efficiencies (±3.6% to 6.1%), the primary ion (S^-) collection and detection efficiencies (+1.0%/−4.1%), and the form factor measurement and integration (+6.8%/−5.7%), for a total instrumental error of ±10.6% to 14.8%. Signal counting statistics add an additional uncertainty of ±1.2% to 6.3%.

A number of instrumental uncertainties can be eliminated if the ratio of the cross section of two channels (channel ratio) is measured instead. While only one channel can be monitored at any particular time with the present apparatus, the signal rates $R(S^+)$, $R(S^{2+})$, and $R(S^{3+})$ can be recorded in rapid succession (1–4 min per product per energy point). The measurements were repeated 16 times to verify that no significant fluctuations in the overlap, ion current, or other such effects were present. The channel ratio is then simply given by $\sigma(S^{n+})/\sigma(S^{m+})=R(S^{n+})/R(S^{m+})$, the accuracy of which depends only on the counting statistics and the collection and detection efficiencies of the signal. Table I reports the results of these measurements.

Table II lists S^+ and S^{2+} absolute cross sections measurements at three photon energies. The channel ratios

TABLE I. Measured channel strength ratios $\sigma(S^{n+})/\sigma(S^{m+})$, reported to 1 SD.

Photon Energy (eV)	Ratio of channel strengths		
	S^{2+}/S^+	S^{3+}/S^+	S^{3+}/S^{2+}
169.911	0.218(16)	0.0182(14)	0.0822(61)
199.866	0.580(41)	0.0867(57)	0.1495(98)
229.820	0.670(49)	0.163(11)	0.252(17)

TABLE II. Measured absolute cross sections (1 SD).

Photon energy (eV)	Cross section (Mb)			
	S^+	S^{2+}	S^{3+}	S^{4+}
170.147	3.30(39)	0.696(85)	0.0585(67)[a]	
200.172	4.18(55)	2.38(31)	0.357(45)[a]	
230.197	3.83(60)	2.31(34)	0.587(84)[a]	~0.023[b]

[a]The S^{3+} cross sections are obtained from the combination of S^+ and S^{2+} cross sections and the channel ratios of Table I.
[b]The S^{4+} signal was found to be about 100 times weaker (within a factor of ~3) than S^{2+} for energies between 230 and 240 eV.

$\sigma(S^{2+})/\sigma(S^+)$ obtained from these measurements are consistent with those in Table I, albeit to lower precision. The very weak signal observed for S^{3+} made direct absolute cross section measurements for that channel prohibitive. Instead, the channel ratios from Table I were used in combination with the S^+ and S^{2+} cross section measurements to obtain two independent (and consistent) estimates of $\sigma(S^{3+})$, the weighted means of which appear in Table II. [The cross section and channel ratio measurements were taken during different experiment runs, resulting in different grating photon-energy calibrations and the 0.24–0.38 eV difference between the tables. Given the bandwidth (300 meV), slow cross section variation, and reported accuracies, the $\sigma(S^{3+})$ estimate is not expected to be significantly affected.] The S^{4+} signal in Fig. 1 was scaled against S^{2+} based on the observed relative count rates of these two species and is expected to be accurate to within a factor of 3.

Higher-statistics scans of the region near the $2p$ threshold are shown in Fig. 2. The photon energy dependence of the signal for S^+, S^{2+}, and S^{3+} is observed to be essentially identical for each channel; this is evidence that all charge

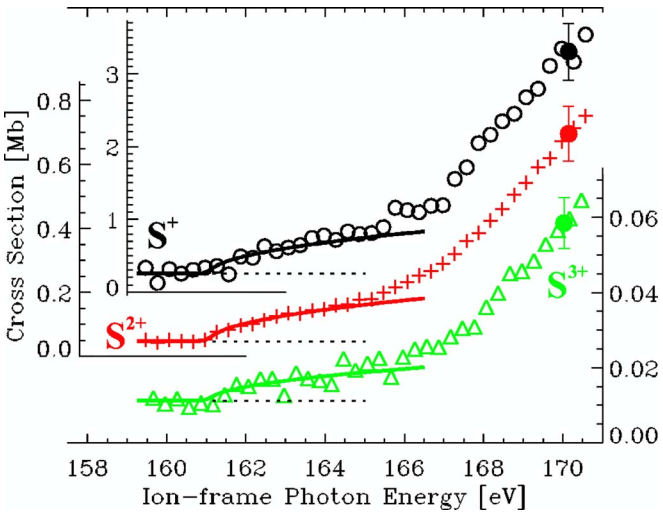

FIG. 2. (Color online) Signal observed from S^+ (◯, left inner scale), S^{2+} (+, left outer scale), and S^{3+} (△, right scale) near the $2p$ threshold. Over this range, the signals from all channels have nearly identical shapes. The curves are Wigner s-wave threshold laws (ε_t=161.04(6) eV, see Ref. [6]).

states near the threshold are sampling the same initial $2p$ photodetachment. It is important to note, however, that the energy difference between the $3s$ and $3p$ valence shells is only $\approx$9 eV, while the ionization potential for S^+ is $V_{ion}(S^+)=23.34$ eV [12]. The two or three sequential Auger processes required to form S^{2+} or S^{3+} from S $2p^{-1}3s^2 2p^5$ are therefore not energetically possible. Either multiple electrons are ejected or excited in the photodetachment process, or the subsequent Auger decay involves the simultaneous ejection of more than one electron (1 down, many out). The former is unlikely to occur until photon energies $\approx V_{ion}(S^+)$ beyond the threshold, and simultaneous multi-Auger processes are required to explain the formation of S^{2+} and S^{3+} near the threshold.

At photoelectron energies sufficiently beyond $V_{ion}(S^+)$, a knockout process [14] (a half-collision between the exiting photoelectron and the atom) can lead to double detachment, and thus explain some of the higher charge state formation. At still higher photon energies, shakeoff processes (arising from electron-electron correlation) may also contribute to multiple ionization. However, comparison with Li photoionization indicates that the ratio of 3 to 2 electron emission remains small in Li ($<1\%$ [15]), as compared to up to 60% observed for S^-. It therefore seems unlikely that shakeoff could account for much of the S^{2+} signal.

A broad feature in the S^+ channel is observed near 175 eV in Fig. 1, and is not present in the other channels. While the onset of decay channels may account for some of the differences in the signal observed between the S^+ and S^{2+} channels, such differences should still be small at these photon energies. The observed increase in the S^+ signal may instead be due to a negative ion resonance just above the threshold that favors decay to S^+.

If we assume that the shape of the S^{2+} signal is representative of the continuum cross section without negative ion resonances we can "remove" the nonresonant signal by subtracting the observed S^{2+} signal, scaled to the S^+ signal using the 230 eV channel ratio ($1/0.67=1.49$). The result shown in Fig. 3 resembles the profile of a shape resonance [17,18]. A Lorentzian line shape yields a good fit to the structure [linecenter=176.4(6) eV and width=20(2) eV], although it is truncated near the threshold. A similar threshold truncation was observed with the $3p\rightarrow 3d$ dipole resonance in Ti^{3+} [16]. In the present case, the structure would most likely be a shape resonance in the d-wave continuum. While a d-wave shape resonance has not been observed previously, p-wave shape resonances are relatively common [17,18]. Theoretical investigations would help to verify the origin of this structure, which may alternatively be due to non-resonant continuum structure differences between the two channels [19].

Figure 4 presents data near the $2s$ detachment threshold using a fine sampling step. An approximate absolute scale was established by comparison with Fig. 1. A clear resonance feature is observed, and is likely due to the $2s\rightarrow 3p$ excitation, which fills the $3p$ shell to form the $2s^{-1}3s^2 3p^6\ ^2S_{1/2}$ state. The cross section increase immediately beyond the resonance (seen in S^{2+} and S^{3+}) is likely due to the onset of the $2s$ threshold, indicating that the S^- $2s^{-1}3s^2 3p^6\ ^2S_{1/2}$ appears as a Feshbach resonance bound below the S $2s^{-1}3s^2 3p^5$ parent state. Similar stabilization of the p valence orbital has been observed with $1s\rightarrow 2p$ excitation in He^- [4] and $4d\rightarrow 5p$ excitation in Te^- [7]. However in those cases, the resonance was only observed in the single-charged product and not in the higher charge states (though there may be a weak coupling to Te^{2+} [7]), while here the resonance couples strongly to product channels up to a charge of at least +3. In fact, the resonance is observed with nearly the same strength in S^{2+} ($\approx$0.4 Mb) as in S^+ ($\approx$0.5 Mb), and about 20% of that strength in S^{3+}. While two (sequential) Auger processes could easily account for S^+ production, here again a

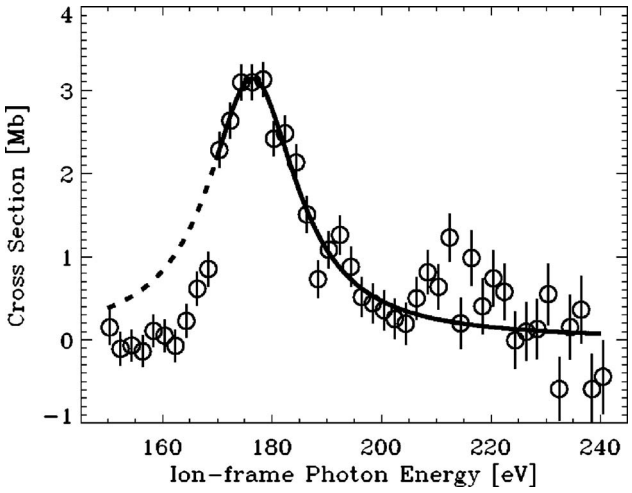

FIG. 3. Possible negative ion resonance in the S^+ channel (extracted from Fig. 1 data, see text). The curve is a Lorentzian fit to the data above 170 eV. The Lorentzian is clearly truncated by the threshold, but otherwise fits the data well.

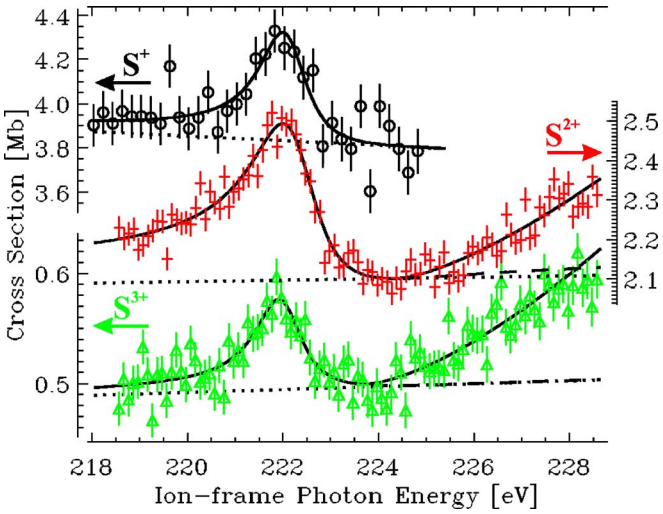

FIG. 4. (Color online) Observed S^+ (◯, top left scale), S^{2+} (+, right scale), and S^{3+} (△, bottom left scale) production following photodetachment near the $2s$ threshold. The data were taken at 0.7(S^+) and 0.3 eV(S^{2+},S^{3+}) spectral resolution. The $2s\rightarrow 3p$ Feshbach resonance is observed near 222 eV, just below the $2s$ threshold. The solid curves are a Fano profile plus p-wave Wigner law. Also shown are the noninterfering continuum background (dotted lines) and the Fano component extended to higher energies (dashed curves).

similar sequential Auger decay process cannot explain S^{2+} and S^{3+} production. To produce S^{2+} and S^{3+}, the decay must proceed via higher order processes such as simultaneous multi-Auger decay or combination of sequential Auger plus shake-up processes.

Fano profile [20] fits yield linecenters of 222.11(20), 222.29(5), and 222.02(20) eV [weighted mean of 222.27(9) eV, including calibration error of 75 meV], widths of 1.2(4), 1.45(4), and 1.1(3) eV [weighted mean of 1.44(4) eV], and shape parameters of −5(5), −2.7(2), and −4(3), respectively, for S^+, S^{2+}, and S^{3+} production. The 2*s* threshold is fit using the Wigner *p*-wave threshold law [9], $\sigma \propto (h\nu - \varepsilon_t)^{1.5}$, where ε_t is the threshold energy. The Wigner law appears to fit the data well here, as we have also observed in a recent study on inner-shell thresholds [6]. However, due to the proximity of the resonance to the threshold, the position is sensitive to the resonance fit parameters, and yields a larger fit uncertainty. Best-fit values of ε_t=224.87(50) and 223.9(9) eV are obtained for S^{2+} and S^{3+}, respectively, yielding a weighted mean of 224.6(5) eV. Using the binding energy of S^- $3s^2 3p^5\ ^2P_{3/2}$ {2.0771029(10) eV [11]}, we obtain the S $2s^{-1}3s^2 3p^5$ core-excited state energy of 222.5(6) eV, which is about 2 eV smaller than the theoretical energy for the L_1M_3 transition of 224.96(72) eV [21]. [The Auger decay lifetime contributes to a shift in the threshold through PCI effects [6]. The decay width of this state is not known, but assuming it is similar to the 2*p* excitation (≈27 meV), a state energy ≈0.2 eV lower would be obtained.] This state has not been directly measured to date, largely due to the extreme difficulty of producing free S atoms.

In summary, we have observed S^+, S^{2+}, S^{3+}, and S^{4+} products from 2*s* and 2*p* photodetachment of S^-. The shapes of the photodetachment cross section for the various products are essentially identical near the threshold, indicating that multi-Auger decay processes are likely the dominant decay mechanism there. At higher energies the spectra differ for different charge states, suggesting significant differences in the decay pathways. Further theoretical input is required for the determination of the dominant decay mechanisms. At 222.27(9) eV, a resonance ≈2 eV below the 2*s* threshold can be attributed to the S^- $2s^{-1}3s^2 3p^6\ ^2S_{1/2}$ state. In the future, comparison with excitations from inner-shell *s* and *d* orbitals into the valence *p* orbital of similar systems (e.g., O^- and Se^-) could yield insight into the decay mechanisms of these highly correlated states. Similar explorations in systems with higher *p*-orbital vacancies would also be of interest. Finally, measurement of the 2*s* detachment threshold energy allowed for the determination of the S $2s^{-1}3s^2 3p^5$ energy, a basic core-excitation transition in S that had previously eluded measurement.

We thank M. Pindzola, S. Manson, and T. Gorczyca for valuable conversations and correspondence, and B. S. Rude and I. Dumitriu for their assistance during some of the experiments. This work was supported by the Department of Energy, Office of Science, BES, Chemical, Geoscience and Biological Divisions. The ALS is funded by the Department of Energy, Scientific User Facilities Division. This material is based in part upon work supported by the National Science Foundation under Grant No. 0140233.

[1] H. Massey, *Negative Ions* (Cambridge University Press, Cambridge, 1976).
[2] T. Andersen, Phys. Rep. **394**, 157 (2004); D. J. Pegg, Rep. Prog. Phys. **67**, 857 (2004).
[3] H. L. Zhou, S. T. Manson, L. Vo Ky, A. Hibbert, and N. Feautrier, Phys. Rev. A **64**, 012714 (2001); J. L. Sanz-Vicario, E. Lindroth, and N. Brandefelt, *ibid.* **66**, 052713 (2002); T. W. Gorczyca *et al.*, *ibid.* **68**, 050703(R) (2003).
[4] R. C. Bilodeau *et al.*, Phys. Rev. Lett. **93**, 193001 (2004).
[5] A. Aguilar *et al.*, Phys. Rev. A **69**, 022711 (2004).
[6] R. C. Bilodeau *et al.*, Phys. Rev. Lett. **95**, 083001 (2005).
[7] H. Kjeldsen, F. Folkmann, T. S. Jacobsen, and J. B. West, Phys. Rev. A **69**, 050501(R) (2004).
[8] H. Kjeldsen *et al.*, J. Phys. B **35**, 2845 (2002).
[9] E. P. Wigner, Phys. Rev. **73**, 1002 (1948).
[10] A. M. Covington *et al.*, Phys. Rev. A **66**, 062710 (2002).
[11] T. Andersen, H. K. Haugen, and H. Hotop, J. Phys. Chem. Ref. Data **28**, 1511 (1999).
[12] Yu. Ralchenko *et al.*, NIST Atomic Spectra Database (ver. 3.0.1). Online: http://physics.nist.gov/asd3 (2005).
[13] Based on similar experiments detecting these charge states: R. A. Phaneuf (private communication).
[14] M. Y. Amusia, *Atomic Photoeffect* (Plenum Press, New York 1990); T. Schneider and J.-M. Rost, Phys. Rev. A **67**, 062704 (2003).
[15] R. Wehlitz *et al.*, Phys. Rev. Lett. **81**, 1813 (1998); M.-T. Huang *et al.*, Phys. Rev. A **59**, 3397 (1999).
[16] S. Schippers *et al.*, J. Phys. B **37**, L209 (2004).
[17] J. R. Peterson, Y. K. Bae, and D. L. Huestis, Phys. Rev. Lett. **55**, 692 (1985).
[18] C. W. Walter, J. A. Seifert, and J. R. Peterson, Phys. Rev. A **50**, 2257 (1994); C. W. Walter and J. R. Peterson, Phys. Rev. Lett. **68**, 2281 (1992); M. Scheer *et al.*, *ibid.* **80**, 684 (1998); R. C. Bilodeau and H. K. Haugen, *ibid.* **85**, 534 (2000); N. D. Gibson *et al.*, Phys. Rev. A **67**, 030703(R) (2003).
[19] There is also some suggestion of structure around 215 eV in the S^+ data of Fig. 3, although the lower signal-to-noise in that region makes it difficult to be conclusive.
[20] U. Fano and J. W. Cooper, Phys. Rev. **137**, A1364 (1965).
[21] R. D. Deslattes *et al.*, X-ray Transition Energies (ver. 1.1). Online: http://physics.nist.gov/XrayTrans (2005).